2004-01-1679

Parametric Study of Transient Turbocharged Diesel Engine Operation from the Second-Law Perspective

C.D. Rakopoulos
National Technical University of Athens

E.G. Giakoumis
Lion Hellas SA, Peugeot Automobiles Distr., Athens

ABSTRACT

A computer analysis is developed for studying the energy and exergy performance of a turbocharged diesel engine, operating under transient load conditions. The model incorporates some novel features for the simulation of transient operation, such as detailed analysis of mechanical friction, separate consideration for the processes of each cylinder during a cycle ("multi-cylinder" model) and mathematical modelling of the fuel pump. The model is validated against experimental data taken from a turbocharged diesel engine, located at the authors' laboratory, operated under transient load conditions. The availability terms for the diesel engine and its subsystems are analyzed, i.e. cylinder for both the open and closed parts of the cycle, inlet and exhaust manifolds, turbocharger and aftercooler. The effect of various dynamic, thermodynamic and design parameters on the second-law transient performance of the engine, manifolds and turbocharger is investigated, i.e. magnitude of applied load, type of connected loading, turbocharger mass moment of inertia, exhaust manifold volume, cylinder wall temperature and aftercooler effectiveness.

Explicit diagrams are given to show how, after a ramp increase in load, each parameter examined affects the second-law properties of all subsystems such as cylinder, heat loss to the walls and exhaust gas availability as well as combustion, exhaust manifold and turbocharger irreversibilities.

It is revealed from the analysis that the in-cylinder (mainly combustion) irreversibilities outweigh all other similar terms for every transient event but with decreasing magnitude when load increases, with the exhaust manifold processes being the second biggest irreversibilities producer with increasing magnitude when load increases.

Design parameters such as cylinder wall insulation or aftercooler effectiveness can have a notable effect on the second-law properties of the engine, despite the fact that their effect on the (thermo)dynamic response is minimal.

INTRODUCTION

Diesel engine simulation modelling has long been established as an effective tool for studying engine performance and contributing to evaluation and new developments. Thermodynamic models of the real diesel engine cycle [1-4] have served as effective tools for complete analysis of engine performance and sensitivity to various operating parameters.

Transient response, especially of turbocharged diesel engines, forms a significant part of their operation and is often characterized by short but serious off-design functions, requiring careful and proper modelling for successful study of the speed response. Transient diesel engine modelling codes and experimental investigation appeared in the early seventies [2,5-7] and continue up to date focusing, among other things, on exhaust emissions [8], variable geometry turbine effects [9] as well as various parametric studies [10-12].

Moreover, during the last two decades, it has become clear that first-law theory alone often fails to provide adequate insight into the engine operations [13-15]. By contrast, second-law (exergy or availability) analysis, with detailed study of what is happening during a process, has contributed a new way of thinking about and studying various thermodynamic engine processes [16-32]. The references include in particular, the ways of irreversibilities production [16,17,21-25], comparison between different burning fuels [24], limited-cooled engine operation [25], parametric study of speed and load effects [26], two-zone modelling [27] as well as spark ignition [28,29] or even Miller engines [30]. Recently, a very detailed review of second-law applications to internal combustion engines has also been published [33].

However, it should be noted that the second-law analysis has always been applied in the past to the steady-state operation of internal combustion engines. The corresponding transient operation case was dealt once in Ref. [34] by the present research group, concerning naturally aspirated engines. In the current paper, the second-law analysis is extended to cover the intrinsically more complicated turbocharged engines transient operation.

For this purpose, a transient diesel engine simulation code has been developed, which incorporates some important novel features to account for the peculiarities of the transient operation. Improved relations concerning (indirect) fuel injection, combustion, dynamic analysis, heat transfer to the cylinder walls, friction modelling, and turbocharger and aftercooler operation have been developed [10-12], which contribute to a more in-depth modelling. Furthermore, a multi-cylinder engine model is incorporated, i.e. one which solves the corresponding differential equations individually for each cylinder, providing a more detailed simulation of the transient processes. The latter issue is important since, during a transient event, considerable differentiations in fuelling from cylinder to cylinder inside the same cycle are observed, particularly during the first cycles.

The experimental investigation was carried out on an MWM TbRHS 518S six-cylinder, IDI (indirect injection), turbocharged and aftercooled, medium-high speed diesel engine of marine duty coupled to a hydraulic brake, located at the authors' laboratory. A high-speed data acquisition system was set up for measuring engine and turbocharger variables performance, under both steady-state and transient operation.

The exergy balance equation was applied to the present diesel engine and all of its subsystems, i.e. compressor, aftercooler, inlet manifold, each cylinder for both the closed and open parts of the cycle, exhaust manifold and turbine. The effect of various dynamic, thermodynamic and design parameters in the second-law transient performance of the engine, manifolds and turbocharger was studied, i.e. type and magnitude of applied load, turbocharger mass moment of inertia, exhaust manifold volume, cylinder wall temperature (profile) and aftercooler effectiveness.

Multiple diagrams are provided to show how, after a ramp increase in load, each parameter examined affects the second-law properties of various subsystems of the engine and the turbocharger, i.e. work, heat loss to the walls and exhaust gas availability as well as combustion, exhaust manifold, turbocharger and aftercooler irreversibilities, given in absolute values and reduced to the incoming fuel exergy or the total irreversibilities.

FIRST-LAW ANALYSIS

Since the present analysis does not include prediction of exhaust gases emissions a single-zone model is used as the basis for the thermodynamic processes evaluation. The fuel is dodecane ($C_{12}H_{26}$) with a lower heating value, LHV=42,500 kJ/kg. Perfect gas behavior is assumed. Polynomial expressions are used for each of the four species (O_2, N_2, CO_2, and H_2O) considered [1], concerning the evaluation of internal energy and specific heat capacities for first-law applications to the engine cylinder contents [1-4,10].

IN-CYLINDER PROCESSES - For the study of the combustion process, the model proposed by Whitehouse and Way is used [1,35]. This model, with separate equations describing the preparation and the reaction rate of the burning process inside the cylinder, has proven its reliability at both steady-state and transient conditions. Moreover, for a more proper simulation of transient response, the combustion modelling applied takes into consideration the continuously changing nature of operating conditions. Thus the constant K_1, in the preparation rate equation of the Whitehouse-Way model, is correlated with the Sauter mean diameter (SMD) of the fuel droplets by a formula of the type $K_1 \propto (1/SMD)^2$ [1]. Here, an empirical expression proposed by Hiroyasu et al. [36] is used for the evaluation of the SMD at each cycle.

The model of Annand [1-4,10,11] is used to simulate heat loss Q_L to the cylinder walls,

$$\frac{dQ_L}{dt} = F\left[g_1 \lambda \, Re^{g_2} \left(T_w - T_g\right)/D + g_3\left(T_w^4 - T_g^4\right)\right] \quad (1)$$

where $F=\pi D^2/4+\pi Dx$ is the surface and x the instantaneous cylinder height in contact with the gas [11], λ is the gas thermal conductivity (W/mK), the Reynolds number Re is calculated with a characteristic speed equal to the mean piston speed and a characteristic length equal to the piston diameter D, and g_i (i=1-3) are constants to be determined after matching with experimental data at steady-state conditions. In particular, for transient engine operation, an "hysterysis" (time lag due to inertia) expression is used to update the wall temperature T_w at each consecutive cycle. The cylinder wall temperature is assumed to remain steady throughout each cycle differentiating from cycle to cycle according to the mean over the cycle fuelling (separately for each cylinder) [9,32].

For the calculation of friction inside each cylinder the method proposed by Rezeka and Henein [37,38,12] is adopted, which describes the non-steady profile of friction torque during each cycle. In this method the total amount of friction is divided into six parts, i.e. ring viscous lubrication, ring mixed lubrication, piston skirt losses, valve train, auxiliaries and loaded bearings. The important aspect about this method is that friction torque varies during each degree crank angle in the engine simulation, unlike the mean fmep (friction mean effective pressure) approaches used so far by all other researchers in the field.

MULTI-CYLINDER MODEL - For the proper simulation of the transient engine performance, a multi-cylinder engine model is developed, i.e. one in which all the governing differential and algebraic equations are solved individually for every one cylinder of the 6-cylinder engine under study. At steady-state operation the performance of each cylinder is essentially the same, due to the steady-state operation of the governor clutch resulting in the same amount of fuel injected per cycle.

At transient operation, on the contrary, each cylinder experiences different fuellings during the same engine cycle due to the continuous movement of the fuel pump rack, initiated by the load or speed change [39]. Thus, they can result in significant differentiations in torque response and finally speed, mainly during the early cycles, so affecting significantly the whole engine operation.

FUEL PUMP OPERATION - The amount of fuel injected per cycle and cylinder is found according to the instantaneous values of engine speed and fuel pump rack position, existing at the point of static injection timing of the particular cylinder. In all the previous transient simulations use was made of steady-state fuel pump characteristics (rack position according to speed and load). In this work a mathematical fuel injection model is used [40] to simulate the fuel pump, providing also the dynamic injection timing and the duration of injection for each transient cycle. This constitutes a vital improvement in transient modelling, since the fuelling characteristics during a transient event differ broadly from the steady-state curves.

DYNAMIC ANALYSIS

ENGINE DYNAMICS - If G_{tot} represents the total system moment of inertia (engine, flywheel and load), then the conservation of energy principle applied to the total system (engine plus load) yields [1,10,11]:

$$T_e(\varphi,\omega) - T_L(\omega) - T_{fr}(\varphi,\omega) = G_{tot}\frac{d\omega}{dt} \qquad (2)$$

where $T_e(\varphi,\omega)$ stands for the instantaneous value of the engine torque, consisting of the gas and the inertia forces torque. In the analysis, the complex (reciprocating and rotating at the same time) movement of the connecting rod is taken into consideration [11]. Also, $T_L(\omega)$ is the load torque,

$$T_L(\omega) = k\omega^s \qquad (2b)$$

where, for the hydraulic brake coupled to the engine examined, s=2. Lastly, $T_{fr}(\varphi,\omega)$ stands for the friction torque, which varies during each cycle and for every cylinder according to the explicit friction analysis based on the Rezeka-Henein method.

TURBOCHARGER DYNAMICS - Accordingly, the dynamic equation for the turbocharger is [5,7,12]:

$$\eta_{mTC}\dot{W}_T - \left|\dot{W}_C\right| = G_{TC}\frac{d\omega_{TC}}{dt} \qquad (3)$$

where $\dot{W}_C$ and $\dot{W}_T$ are the instantaneous values for the compressor and turbine power, respectively, while the turbocharger mechanical efficiency η_{mTC} is mainly a function of its speed.

GOVERNOR DYNAMICS - To find the instantaneous fuel pump rack position z which is initiated by the mechanical governor clutch movement, during the transient operation, a second order differential equation is used [2,5,12]:

$$\frac{d^2z}{d\varphi^2} = c_1\frac{dz}{d\varphi} + c_2 z + c_3 z\omega^2 + c_4\omega^2 + c_5 \qquad (4)$$

with constants c_i (i=1-5) derived after calibration against experimental data under transient conditions.

SECOND-LAW ANALYSIS

GENERAL DESCRIPTION - The exergy or availability of a system in a given state is defined as the maximum reversible work that can be produced through interaction of the system with its surroundings as it reaches thermal, mechanical and chemical equilibrium [13-17,19,23]. In this study, only thermal and mechanical availability terms are taken into account, while chemical availability is involved only in the reactions of fuels to form combustion products.

Application of the exergy balance equation to the diesel engine subsystems, on a °CA basis, yields the relations to be given in the succeeding paragraphs [13,26,31]. Indices 1 to 7 refer to the strategic points locations indicated on the schematic arrangement of the engine depicted in Figure 1.

CYLINDER - For the cylinder, we have:

$$\frac{dA_j}{d\varphi} = \frac{\dot{m}_{4j}b_4 - \dot{m}_{5j}b_{5j}}{6N} - \frac{dA_w}{d\varphi} - \frac{dA_L}{d\varphi} + \frac{dA_{fb}}{d\varphi} - \frac{dI}{d\varphi} \qquad (5)$$

with $\dot{m}_{4j}$ the incoming flow rate from the inlet manifold and $\dot{m}_{5j}$ the outgoing one to the exhaust manifold for the particular cylinder j according to the energy analysis;

$$\frac{dA_w}{d\varphi} = (p_{5j} - p_o)\frac{dV}{d\varphi} \qquad (6)$$

is the work transfer, where $dV/d\varphi$ is the rate of change of cylinder volume with crank angle [10] and p_{5j} the instantaneous cylinder pressure;

$$\frac{dA_L}{d\varphi} = \frac{dQ_L}{d\varphi}(1 - \frac{T_o}{T_{5j}}) \qquad (7)$$

is the heat transfer to the cylinder walls with $dQ_L/d\varphi$ given by the Annand correlation (Equation (1)), and T_{5j} the instantaneous cylinder gas temperature;

$$\frac{dA_{fb}}{d\varphi} = \frac{dm_{fb}}{d\varphi} a_{fch} \qquad (8)$$

is the injected fuel availability, with a_{fch} being the (chemical) availability associated with burning of liquid hydrocarbon fuels of the type C_mH_n and given by Moran [13]:

$$a_{fch} = LHV\left(1.04224 + 0.11925\frac{n}{m} - \frac{0.042}{m}\right) \qquad (8b)$$

For the present analysis, m=12, n=26 and a_{fch}=1.064LHV. The fuel burning rate $dm_{fb}/d\varphi$ is calculated, for each computational step, with the use of the Whitehouse-Way model. The term on the left hand side of Equation (5) is expressed explicitly as:

$$\frac{dA_j}{d\varphi} = \frac{dU}{d\varphi} + p_o\frac{dV_j}{d\varphi} - T_o\frac{dS_j}{d\varphi} - \frac{dG_{oj}}{d\varphi} \qquad (9)$$

representing the change in the availability of the contents of cylinder j under consideration. Details about the derivation of terms U (internal energy), S (entropy), and G (Gibbs free enthalpy) can be found in Ref. [26]. The terms b_4 and b_5 in Equation (5) refer to the flow availability of the incoming and the outgoing cylinder mass flow rate, respectively, defined as [13]:

$$b = h - h_o - T_o(s - s_o) \qquad (10)$$

The term $dI/d\varphi$ in Equation (5) is the rate of irreversibility production within the cylinder which consists mainly of the combustion term, while the contribution of inlet-valve throttling and mixing of the incoming air with the cylinder residuals is of lesser importance.

COMPRESSOR - For the compressor there exists no control volume, so that the exergy balance equation reads:

$$\frac{\dot{m}_1 b_1 - \dot{m}_2 b_2}{6N} + \frac{\dot{W}_C}{6N} = \frac{dI_C}{d\varphi} \qquad (11)$$

with $\dot{m}_1 = \dot{m}_2$ the charge air flow rate.

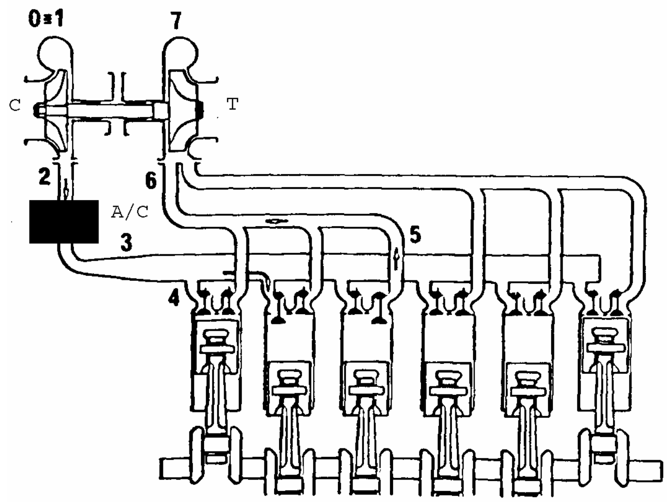

Figure 1. Schematic arrangement of the diesel engine, manifolds, turbocharger and aftercooler.

AFTERCOOLER - For the aftercooler, similarly, the exergy-balance equation is:

$$\frac{\dot{m}_2 b_2 - \dot{m}_3 b_3}{6N} - \Delta A_{cw} = \frac{dI_{AC}}{d\varphi} \qquad (12)$$

where b_2 is the flow availability at the compressor outlet=aftercooler inlet, b_3 the flow availability at the aftercooler outlet=inlet manifold inlet, and

$$\Delta A_{cw} = \frac{\dot{m}_{cw} c_{pcw}\left[T_{cw-out} - T_{cw-in} - T_o \ln\left(\frac{T_{cw-out}}{T_{cw-in}}\right)\right]}{6N} \qquad (13)$$

is the increase in the availability of the cooling medium [13] having mass flow rate $\dot{m}_{cw}$, specific (mass) heat capacity c_{pcw}, initial temperature entering the aftercooler T_{cw-in} and final temperature leaving the aftercooler T_{cw-out}. Here, the irreversibilities account for the loss of exergy due to the transfer of heat to a cooler medium.

INLET MANIFOLD - For the inlet manifold, the exergy balance equation is:

$$\frac{dA_{im}}{d\varphi} = \frac{\dot{m}_3 b_3 - \sum_{j=1}^{6} \dot{m}_{4j} b_{4j}}{6N} - \frac{dI_{im}}{d\varphi} \qquad (14)$$

where b_4 is the flow availability at the intake-manifold and j=1-6 the cylinder exchanging mass with the inlet manifold found from the energy analysis at each degree crank angle. The term for irreversibilities $dI_{im}/d\varphi$ accounts mainly for the mixing of incoming air with the intake manifold contents.

EXHAUST MANIFOLD - For the exhaust manifold, the exergy-balance equation is:

$$\frac{dA_{em}}{d\varphi} = \frac{\sum_{j=1}^{6} \dot{m}_{5j} b_{5j} - \dot{m}_6 b_6}{6N} - \frac{dI_{em}}{d\varphi} + \frac{dA_{Lem}}{d\varphi} \quad (15)$$

where index 6 identifies the exhaust manifold state. The term

$$\frac{dA_{Lem}}{d\varphi} = \frac{dQ_{Lem}}{d\varphi}\left(1 - \frac{T_o}{T_6}\right) \quad (16)$$

accounts for heat losses at the exhaust manifold, where T_6 is the instantaneous temperature of the manifold contents. The term $dI_{em}/d\varphi$ is the irreversibility rate in the exhaust manifold, which arises from throttling across the exhaust valve, mixing of cylinder exhaust gases with manifold contents and friction along the manifold length. The $dA/d\varphi$ terms given in the previous equations for the cylinder and the manifolds are evaluated according to Equation (9); for unsteady operations they do not sum to zero (as they do for steady-state operation) at the end of a full cycle of the working medium. Their respective cumulative values $\int (dA/d\varphi) d\varphi$ are, however, small (not more than 0.40% of the incoming fuel's exergy) compared to the other availability terms, due to the large total moment of inertia of the examined engine-brake system, which slows down the reaction of the fuel pump rack and consequently the speed response of the engine.

TURBINE - For the turbine, the exergy balance equation is:

$$\frac{\dot{m}_6 b_6 - \dot{m}_7 b_7}{6N} - \dot{W}_T = \frac{dI_T}{d\varphi} \quad (17)$$

with 7 denoting the state of the gases leaving to the atmosphere from the turbine.

COMPUTER SIMULATION

All the equations for the energy and exergy simulation are solved for every ¼ ^oCA for the closed part of each cycle, or every ½ ^oCA for the open part. The dynamic ones are solved once every degree crank angle for the diesel engine and every 120 ^oCA for the turbocharger. These computational steps were found to be adequate for the particular engine-turbocharger-brake configuration which is characterized by a high mass moment of inertia.

EXPERIMENTAL FACILITIES AND MEASUREMENTS

The objective of the experimental test bed developed was to validate the transient performance of the engine simulation. To accomplish this task the engine was coupled to a hydraulic brake (dynamometer). The experimental investigation was conducted on an MWM TbRHS 518S, 6-cylinder, turbocharged and aftercooled, indirect injection (IDI), medium-high speed diesel engine of marine duty. The basic data for the engine, turbocharger and brake are given in Table 1.

Table 1. Basic data for engine, turbocharger, and dynamometer.

Engine Model and Type	MWM TbRHS 518S, In-line, 6-cyl., 4-stroke, compression ignition, IDI, turbocharged, aftercooled, marine duty
Speed Range	1000-1500 rpm
Bore/Stroke	140 mm/180 mm
Compr. Ratio	17.7
Max. Power	320 HP (236 kW) @ 1500 rpm
Max.Torque	1520 Nm @ 1250 rpm
Intake Valve Open./Closure	51 ^oCA before TDC/60 ^oCA after BDC
Exh. Valve Open./Closure	64 ^oCA before BDC/47 ^oCA after TDC
Fuel Pump	Bosch PE-P series, in-line, 6-cylinder with mechanical governor Bosch RSUV 300/900
Brake	Schenck U1-40, hydraulic brake
Total Moment of Inertia	15.60 kg m^2
Turbocharger Model & Type	KKK M4B 754/345, Single-stage, centrifugal compressor, Single-stage, twin entry, axial turbine
T/C Moment of Inertia	7.5×10^{-4} kg m^2

The investigation of transient operation was the next task. Since the particular engine is one with a relatively small speed range, mainly load changes (increases), with constant governor setting were examined. In particular, for the transient tests conducted the initial speed was 1180 or 1380 rpm and the initial load 10% of the engine full load. The final conditions for the transient events varied from 47 to 95% of the engine full load as analyzed in detail in Ref. [12].

RESULTS AND DISCUSSION

A typical example of a conducted transient experiment is given in Figure 2. Here, the initial load was 10% of the full engine load at 1180 rpm. The final load applied was almost 75% of the full engine load, which corresponds to a brake load increase of 650%; it was applied in 0.2 seconds.

The application of the final load was effected by the movement of the brake control lever (this task lasted 0.2 seconds), which in turn increased the amount of water inside the brake by appropriately increasing the active surface of the inlet tube. However, this hydraulic brake is characterized by a high mass moment of inertia, in the order of 5.375 kg m^2, resulting in long, abrupt and non-linear actual load-change profile. The actual duration of the load application was accounted for in the simulation model by increasing the load application time. The non-linear character of the load application though, which could not be accounted for in the simulation, is responsible for the difference observed between experimental and simulated results during the early cycles in Figure 2. On the other hand, the matching between experimental and predicted transient responses is satisfactory for both engine and turbocharger variables (engine speed, maximum pressure for main chamber, fuel pump rack position and boost pressure) as regards the final conditions.

Figure 3 shows the response of the in-cylinder exergy terms, viz., work, heat loss to the walls, exhaust gas and irreversibilities as a function of the engine cycles. All of these terms are cumulative values (J) over each cycle (for cylinder No 1 of the engine). The exergy term for work and heat loss to the walls increase with the increase in fuelling as a function of the engine cycles, because of increases in the charge temperature resulting from increases of the injected fuel quantity and accompanying fuel-air equivalence ratios. Similar results hold for the exhaust gas from the cylinder term and for the irreversibilities term. Cylinder irreversibilities consist of combustion ones (almost 95% of the total), inlet and exhaust ones.

Figure 4 concentrates on the irreversibilities terms of the various subsystems, reduced now to the total irreversibilities. Here, is shown how in-cylinder as well as inlet manifold, exhaust manifold, aftercooler, compressor and turbine irreversibilities develop according to the evolution of the engine cycles. The relative importance of the in-cylinder irreversibilities decreases as the transient event develops, because with the increase in fuelling the degradation of the fuel chemical availability to the exhaust gas decreases (a fact responsible for the main part of combustion irreversibilities) as the gas temperatures reach higher values. The inlet-manifold irreversibilities constitute a very small percentage of the total ones (not greater than 3.2% and with decreasing relative importance during the transient event), whereas those of the exhaust manifold increase substantially from cycle 10 where the main increase in the injected fuel quantity occurs, reaching as much as 15% of the total irreversibilities at cycle 31. Turbocharger irreversibilities increase during the transient event due to the increase in both compressor and turbine pressure and temperature, accounting for 4.7% of the total irreversibilities at cycle No 28. The compressor irreversibilities outweigh the turbine ones, except for the first cycles where the turbine isentropic efficiency is lower. Aftercooler irreversibilities never exceed 0.47% of the total ones (cycle No 30), proving the low importance of this process. It is also interesting to note, that the cycle where the maximum (or minimum) percentage occurs differs for every subsystem. This is due to the different «inertia» of each subsystem, which differentiates also its transient response.

First-law properties (such as torque or power) have a rather straightforward mathematical meaning. Second-law properties, on the other hand, can be interpreted in different ways according to the chosen property for reduction, giving conflicting results. This is shown in Figure 5 where the in-cylinder irreversibilities response is depicted for the nominal load change. Here, the in-cylinder irreversibilities are given in J but also reduced to the incoming fuel exergy and reduced to the total (engine plus turbocharger) irreversibilities. The above mentioned conflict in meaning and magnitude is highlighted in this figure, where it is shown that the in-cylinder irreversibilities increase as the transient event (load increase) proceeds but their relative importance according to the total irreversibilities decreases, and their relative importance according to the incoming fuel availability decreases also but now at a much greater rate. Then, it is imperative to choose carefully the most representative properties for investigation in each case concerned.

In the following diagrams the effect of various dynamic, thermodynamic and design parameters on the engine and turbocharger second-law transient response will be investigated. For all cases analysed below, unless otherwise stated, the following assumptions are valid:

1. The initial load is 10% of the engine's full load at the initial speed of 1180 rpm.
2. A 650% load-change is applied in 1.3 sec (real load application time) corresponding to a 10-75% load-change.
3. The loading type is quadratic (hydraulic brake, s=2 in Equation (2b)).
4. The temperature of the cylinder walls ranges from 400 K (at the initial operating point of 10% load) to 500 K (100% loading) in the vicinity of 1180 rpm engine speed, according to the current fuelling conditions. This temperature is assumed to remain steady during each cycle differentiating from cycle to cycle.

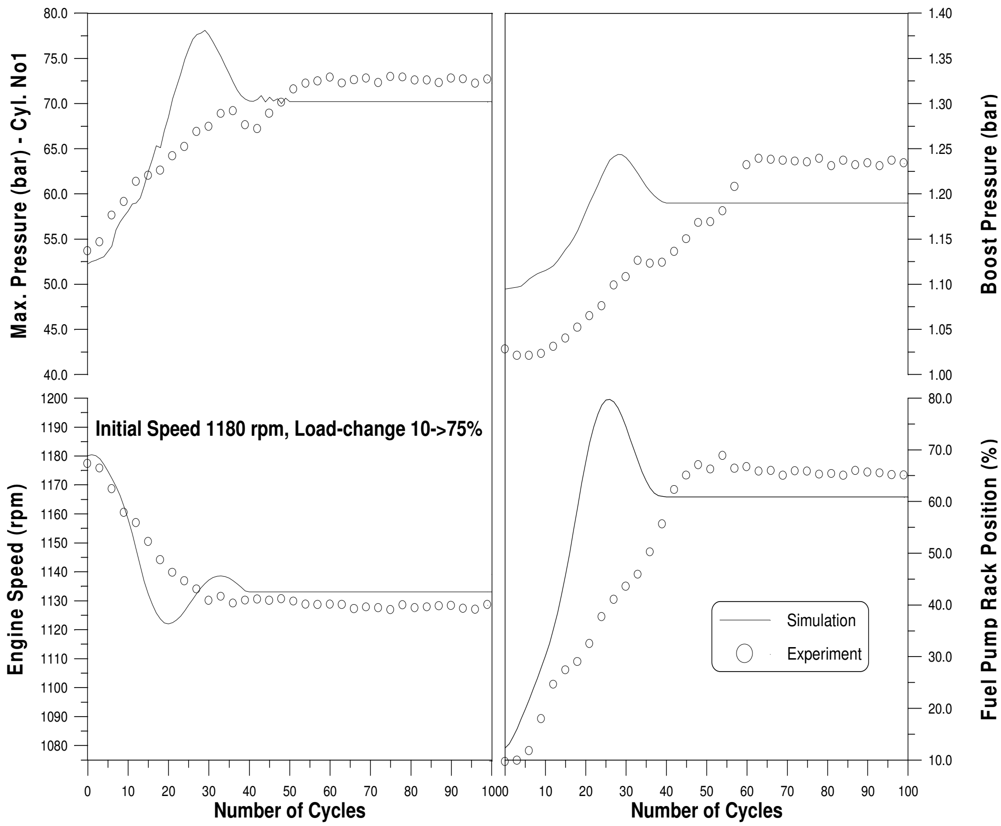

Figure 2. Experimental and predicted transient response to an increase in load.

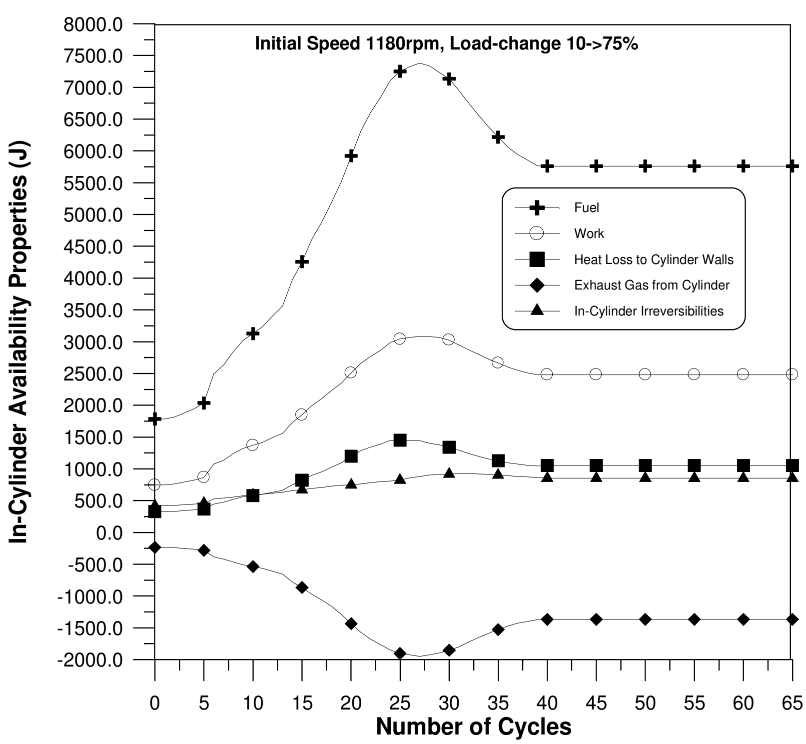

Figure 3. Response of in-cylinder availability properties to an increase in load.

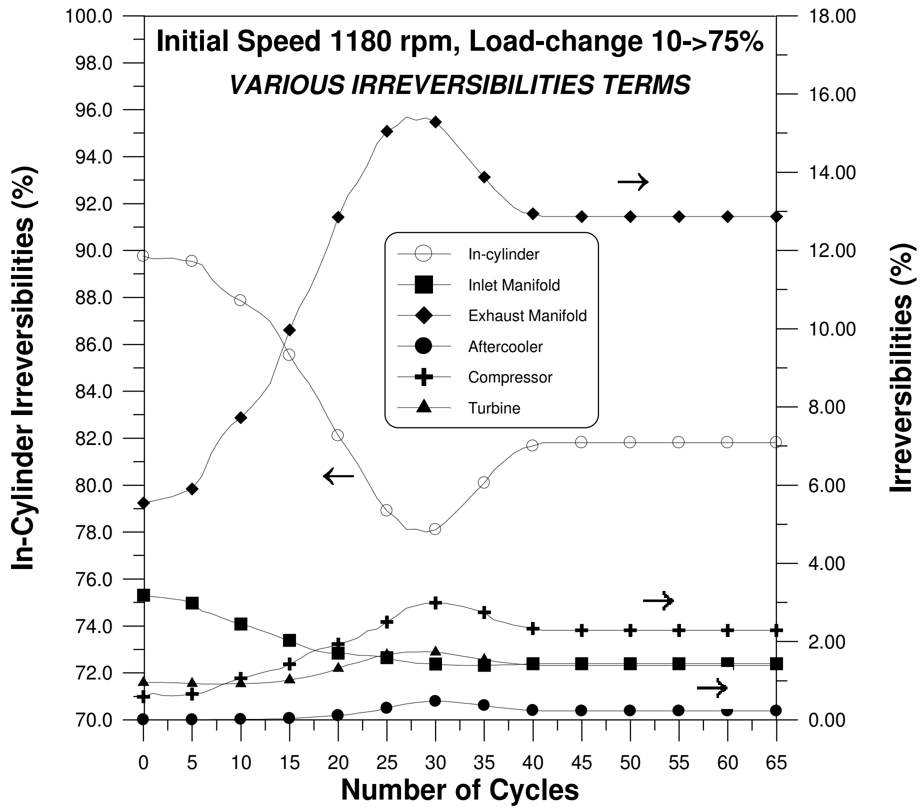

Figure 4. Response of various diesel engine and its subsystems irreversibilities terms, reduced to the total irreversibilities, to an increase in load.

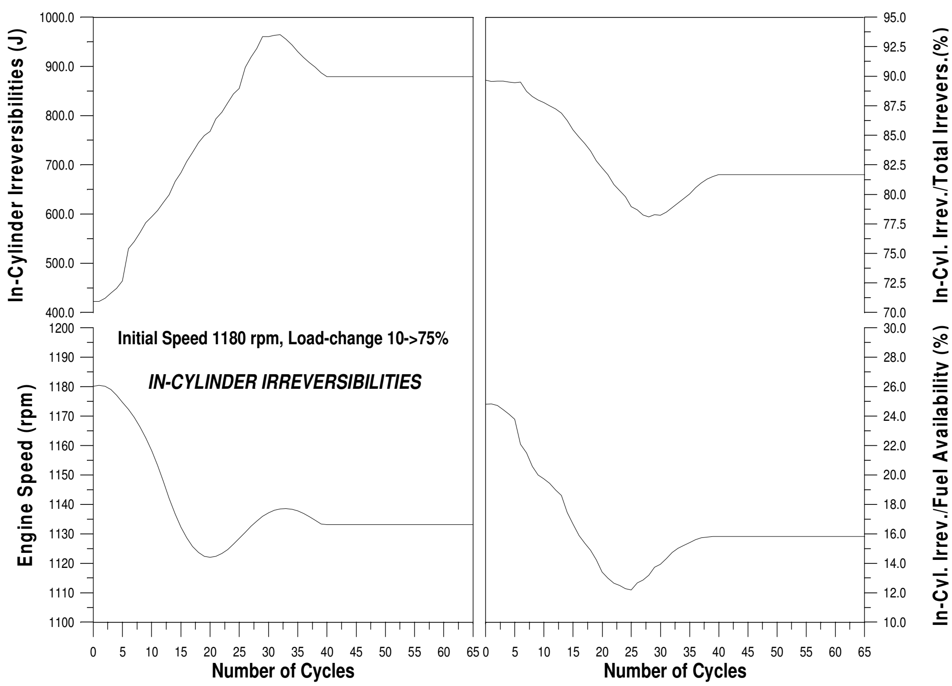

Figure 5. Response of in-cylinder irreversibilities to an increase in load.

Multiple diagrams will be used to highlight each parameter's effect. In all diagrams the engine speed and the in-cylinder irreversibilities reduced to the incoming fuel exergy will be given. The rest of the sub-diagrams will depict a different property each time both in absolute value and reduced value. This property has been carefully chosen for every case to be one closely related to the examined parameter (for example exhaust manifold irreversibilities when the effect of the exhaust manifold volume is examined).

Figure 6 investigates the effect of the magnitude of the applied load on the second-law transient response. Apart from the nominal case (650% load-change), the 400% and the 900% load-changes are also studied. The interesting property chosen here for depiction, along with the engine speed and the in-cylinder irreversibilities, is the brake work produced by cylinder No 1. It is obvious from Figure 6 that a greater applied load leads to a decrease in the reduced in-cylinder irreversibilities (cf. Figure 5). The work on the other hand, although increasing in J with the increase in the applied load, decreases slightly when it is reduced to the injected fuel availability mainly due to greater increases in the mechanical friction associated with higher loads.

Figure 7 focuses on the effect of the type of the load connected to the engine. The cases with linear load (e.g. electric brake) and rigid load are studied here along with the nominal case of quadratic load. The exergy term of the exhaust gases from cylinder was chosen as the interesting property. The lower the exponent 's' in Equation (2b), which means a more rigid connected load, the greater the engine speed droop (difference between initial and final engine speed), which in turn leads to greater fuel pump rack position and consequently to an increase in the injected fuel quantity, thus decreasing the in-cylinder irreversibilities reduced to the fuel exergy. On the other hand, a more rigid loading increases the amount in J of the availability term of the exhaust gas from the cylinder (absolute value) due to the increase in the in-cylinder temperatures resulting from the increased fuelling, while the respective one reduced to the incoming fuel exergy term increases as an absolute value too. The latter fact implies that with the increase in fuelling the exhaust gases availability increase at a greater rate than the respective fuel exergy.

Figure 8 concentrates on the effect of the turbocharger mass moment of inertia. Here the turbine irreversibilities were chosen as the interesting property. Two cases are examined apart from the nominal one. In the first case the T/C inertia is one fifth of the nominal inertia and in the second one its value is 10 times the nominal one. The lower the turbocharger mass moment of inertia the lower the speed droop (notice the pulsating engine speed recovery), leading to greater reduced in-cylinder irreversibilities. The turbine irreversibilities (in J) increase slowly during the transient event with increasing T/C mass moment of inertia due to the slow T/C pressure and temperature build up; they reach lower values compared to the case with lower T/C mass moment of inertia. Nonetheless, the turbine irreversibilities reduced to the total ones increase with increasing T/C inertia (although the value never exceeds 2% of the total irreversibilities), pinpointing the above mentioned "conflict" in the results of the second-law analysis.

Figure 9 focuses on the effect of the cylinder wall temperature on the exergy response of the engine. The heat loss to the cylinder walls availability was chosen here as the interesting property for depiction, along with the reduced in-cylinder irreversibilities. In the first case the cylinder wall temperature is 400 K remaining steady throughout the transient event. In the second case (nominal) the wall temperature is assumed to vary from 400 to 500 K according to the engine (steady-state) fuelling and in the third case the cylinder wall is assumed to remain steady at 600 K; the latter resembles the "adiabatic" or low heat rejection engine. An increasing wall temperature leads to greater gas temperatures inside the cylinder, which in turn lower the in-cylinder irreversibilities reduced to the fuel exergy (due to a lower degradation of the fuel exergy to the "hotter" exhaust gases), while the exergy of the heat loss to the cylinder walls increases both in J and reduced to the injected fuel exergy. Notice that for the "adiabatic" wall case the reduced to the fuel exergy in-cylinder irreversibilities drop up to 7.5% compared to the 12% for the nominal case, denoting how favorable, according to the second-law perspective, this configuration is. Although the cylinder wall temperature effect on the engine speed response is minimal, its second-law magnitude is notable leading to significant variations in the exergy terms thus highlighting the importance of the second-law perspective.

Figure 10 investigates the effect of the aftercooler effectiveness on the second-law response. Double and half values for the aftercooler effectiveness were chosen here for study, with the aftercooler irreversibilities chosen to be the interesting property for depiction. The engine recovery remains almost totally unaffected by the magnitude of the aftercooler effectiveness, something however not applicable to the second-law properties. An increasing A/C effectiveness decreases the charge air temperature leading to increased reduced in-cylinder irreversibilities due to greater degradation of the fuel exergy to "cooler" exhaust gases. As regards the aftercooler irreversibilities, although their absolute value remains of a very small magnitude, there exists a significant differentiation as regards both the values in J and the ones reduced to the total irreversibilities. It is made obvious from Figure 10 that the combined effect of the incoming and outgoing flow availabilities, described in Equation (12), leads to an increase in the aftercooler irreversibilities with the increase in its effectiveness.

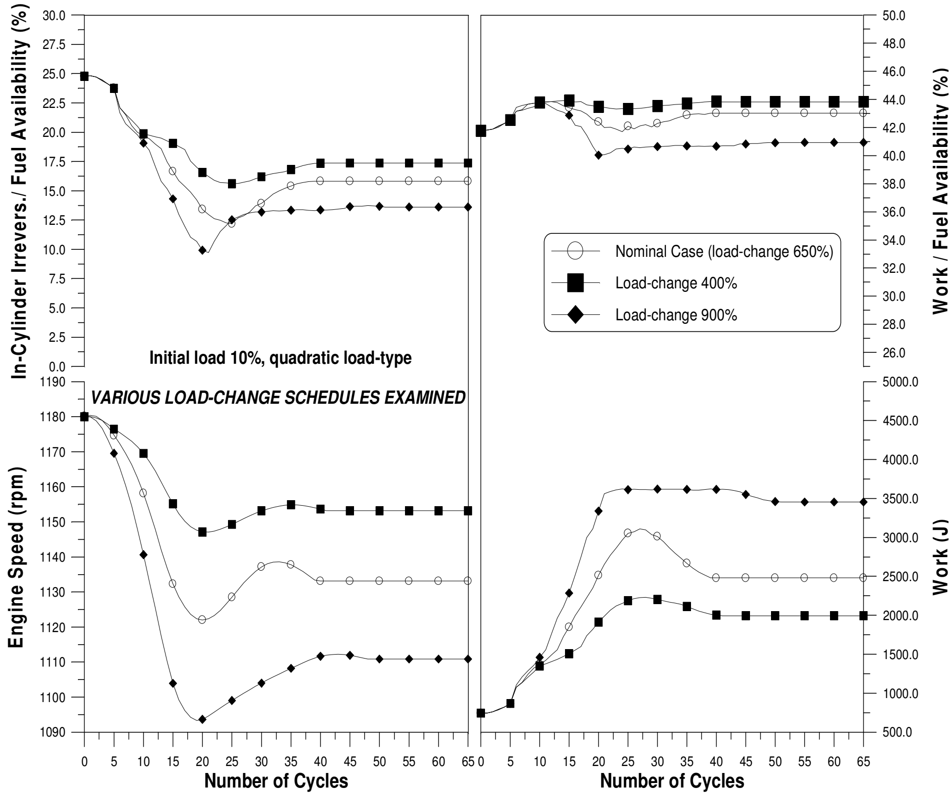

Figure 6. The effect of magnitude of applied load on the second-law transient response.

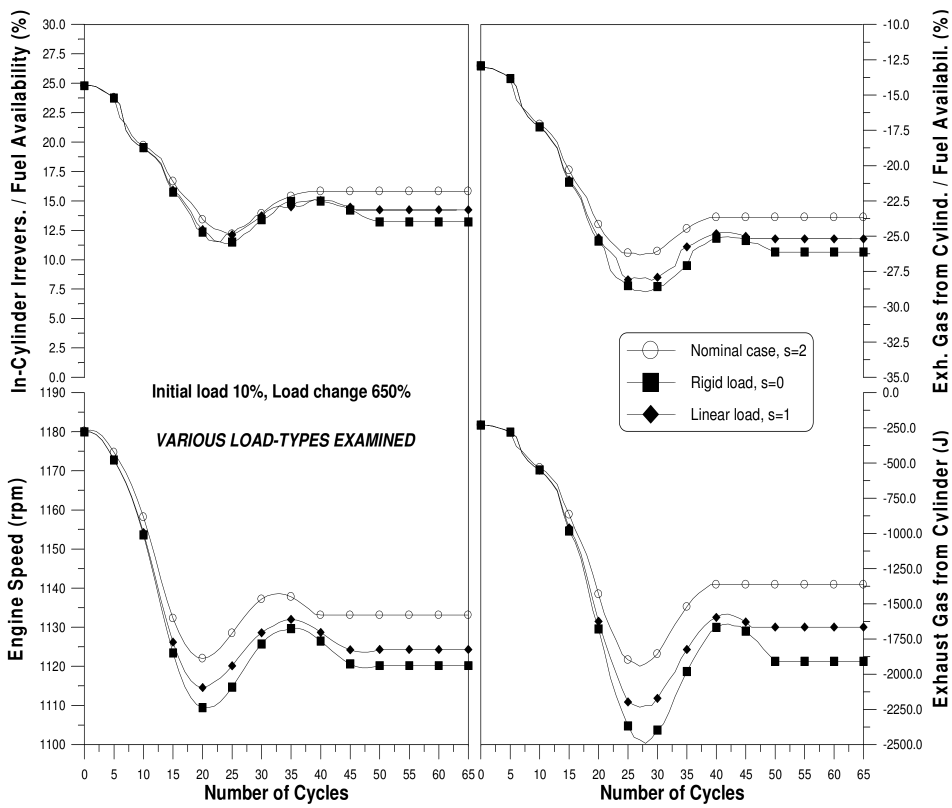

Figure 7. The effect of loading type on the second-law transient response.

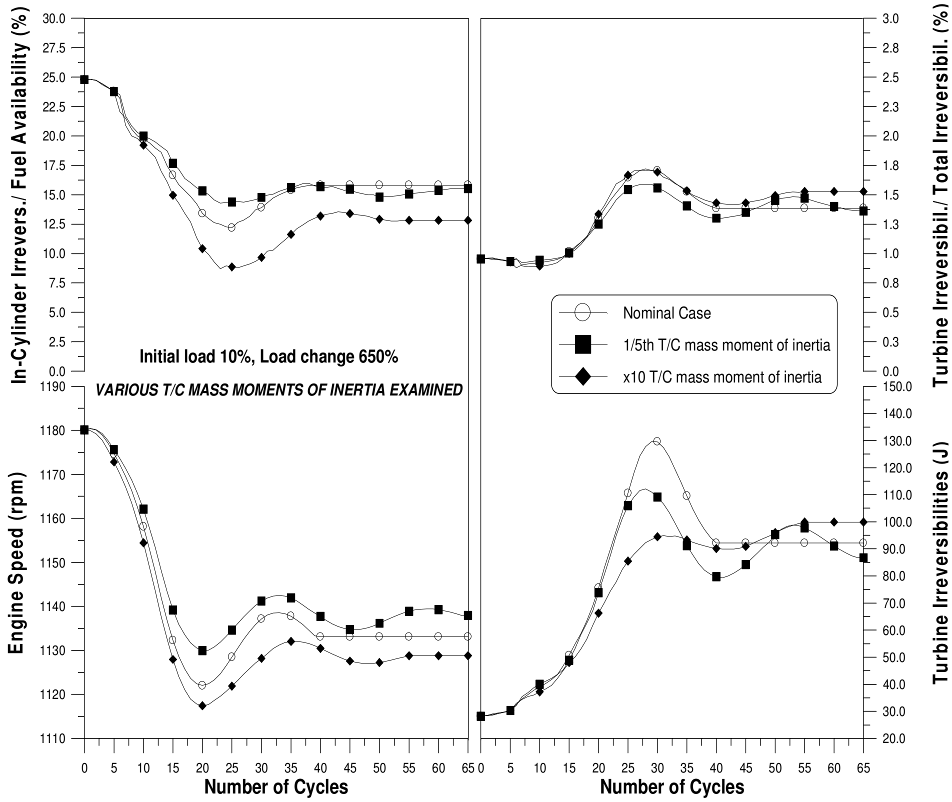

Figure 8. The effect of turbocharger mass moment of inertia on the second-law transient response.

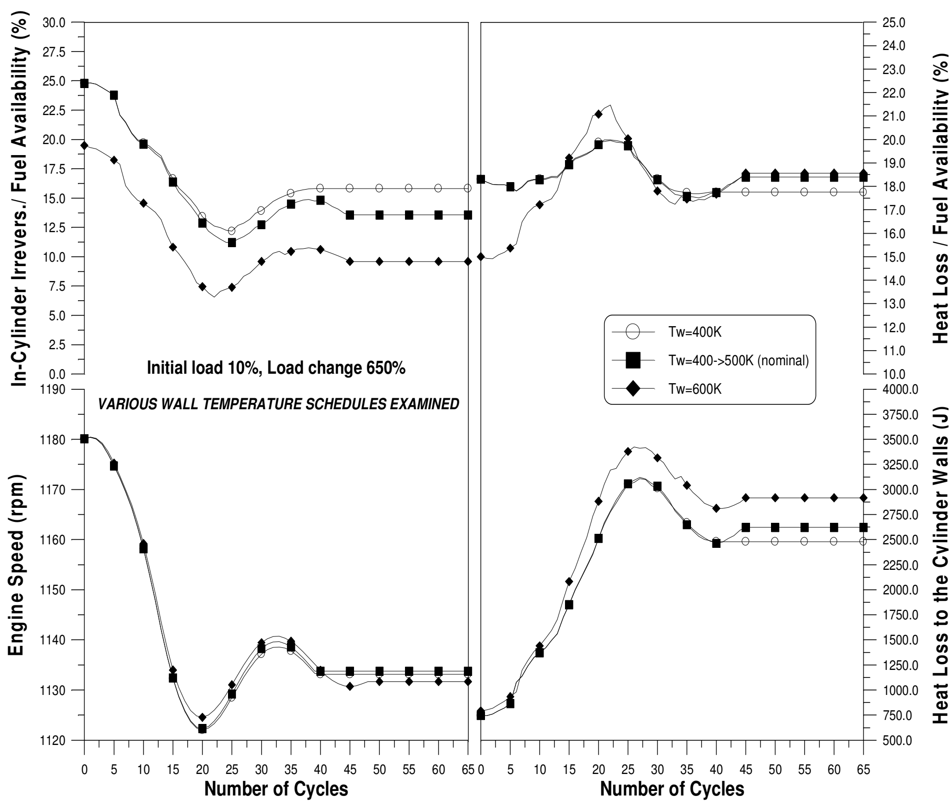

Figure 9. The effect of cylinder wall temperature on the second-law transient response.

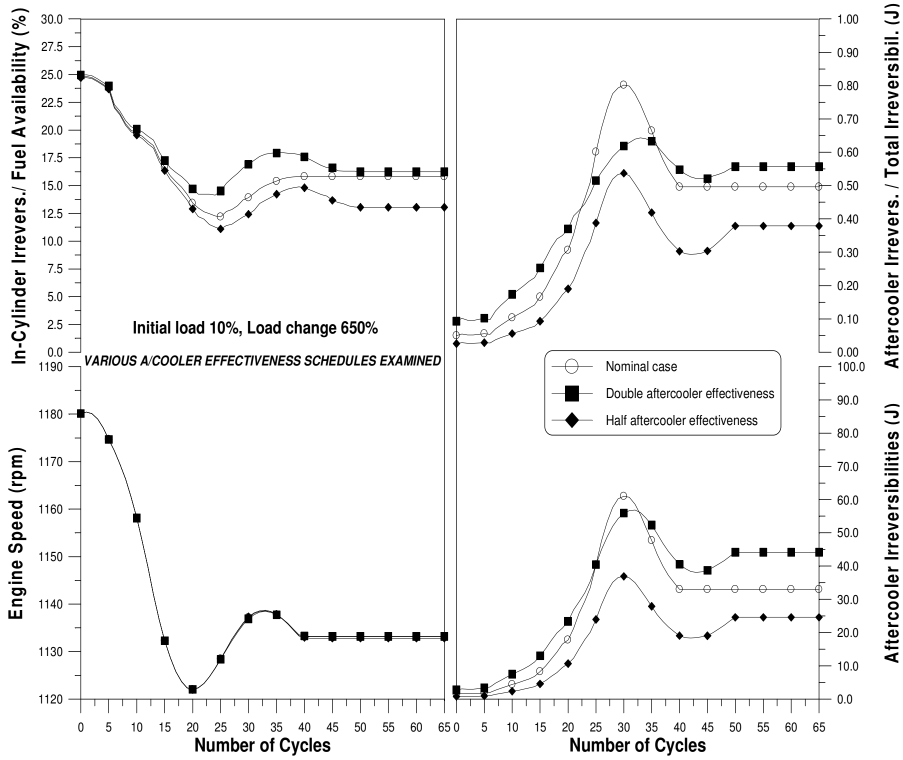

Figure 10. The effect of aftercooler effectiveness on the second-law transient response.

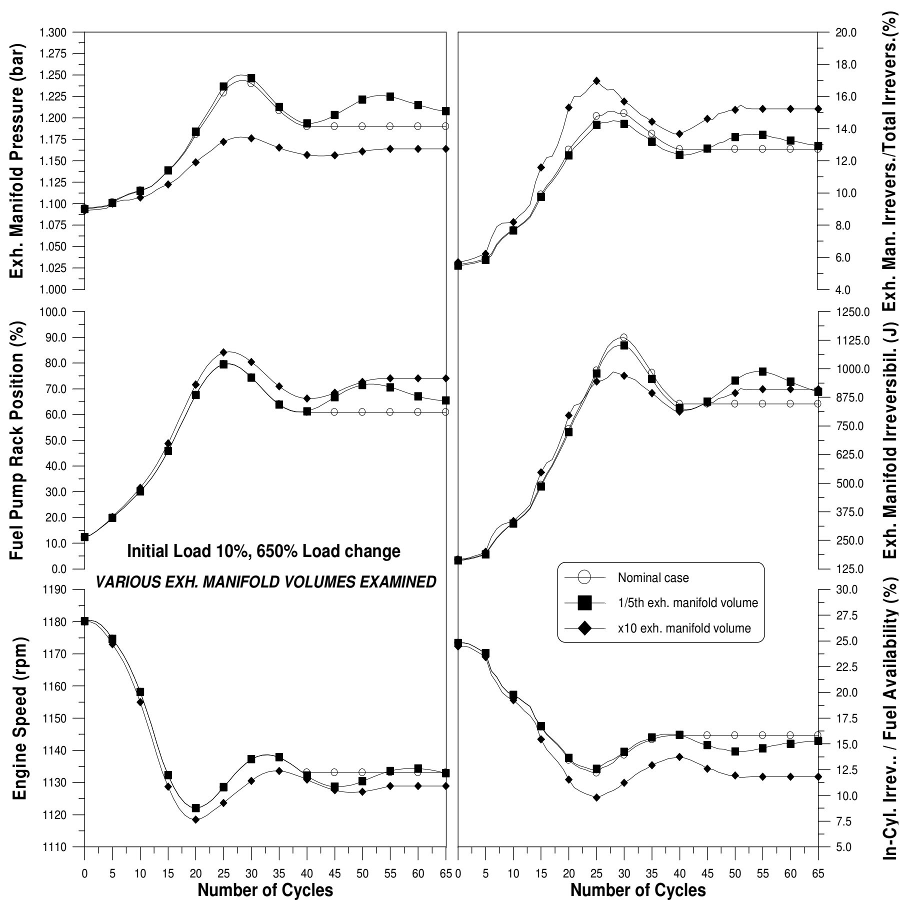

Figure 11. The effect of exhaust manifold volume on the second-law transient response.

Figure 11 investigates the effect of the exhaust manifold volume on the second-law response of the engine. A large manifold volume (resembling a constant pressure turbocharging system) leads to slow engine speed recovery, thus increasing the injected fuel quantity and so decreasing the relative importance of the in-cylinder irreversibilities. On the other hand the low pressures and temperatures in a large exhaust manifold lead to reduced manifold irreversibilities (in J) compared to the case with lower exhaust manifold volumes, whereas the relative importance of the manifold irreversibilities increases (cf. Figure 8 for the great T/C mass moment of inertia effect).

CONCLUSION

A detailed second-law analysis has been carried out on a 6-cylinder, turbocharged diesel engine to study the effect of various dynamic, thermodynamic and design parameters on the second-law response of all engine subsystems during transient operation commencing from a low load. The model's energy results were confirmed with experimental tests. Explicit diagrams were given to highlight each second-law property response. Various properties reduced (to the incoming fuel exergy or the total irreversibilities) were studied. The analysis revealed the following:

- Cylinder (mainly combustion) is by far the biggest irreversibilities producer whatever the load schedule (but with decreasing importance with increasing load), with the exhaust manifold irreversibilities accounting for as much as 15% of the total ones for high loads. On the other hand, aftercooler irreversibilities never exceed 0.5% of the total ones.
- Certain design parameters such as the cylinder wall temperature or the aftercooler effectiveness can have a significant effect on the second-law response of the engine, although their impact on the first-law transient results is minimal. This remark best pinpoints the different perspective of processes that the second-law theory introduces compared to the first-law one.
- All the parameters which lead to slow engine speed recovery (such as large exhaust manifold volume or high T/C mass moment of inertia) result in increased fuel injected quantities and thus decreased in-cylinder irreversibilities when reduced to the fuel exergy. Similar remarks hold for the parameters (such as high cylinder wall temperature or decreased aftercooler effectiveness) which lead to increased charge air temperatures.
- The greater the applied load, the greater the in-cylinder irreversibilities (in J) but with decreasing reduced value. The same applies to the more rigid load-types also.
- Various second-law properties (such as work, heat loss to the wall, exhaust gases, various subsystems irreversibilities) differentiate by a lot during a transient event, but with an often conflicting magnitude when the same properties are reduced to the incoming fuel exergy or the total irreversibilities.

The application of the aforementioned analysis to the engine design is an important subject. The particular study spotted specific engine processes and parameters apart from the well known in-cylinder irreversibilities (such as the exhaust manifold irreversibilities, the cylinder wall insulation and the aftercooler effectiveness) which could, according to the exergy analysis, improve the engine processes. For example, the use of insulated cylinder wall is a proposal for better engine performance according to (transient) second-law analysis. A detailed optimization based on both the first and second-law is needed for the establishment of any such aspects.

REFERENCES

1. Benson, R.S. and Whitehouse, N.D., "*Internal Combustion Engines*", Oxford, Pergamon Press, 1979.
2. Horlock, J.H and Winterbone, D.E., "*The Thermodynamics and Gas Dynamics of Internal Combustion Engines, Vol. II*", Oxford, Clarendon Press, 1986.
3. Rakopoulos, C.D. and Hountalas, D.T., "Development and validation of a 3-D multi-zone combustion model for the prediction of DI diesel engines performance and pollutants emissions", SAE paper No 981021, SAE Transactions, Journal of Engines, Vol. 107, pp. 1413-1429, 1998.
4. Rakopoulos, C.D. and Hountalas, D.T., "Development of new 3-D multi-zone combustion model for indirect injection diesel engines with a swirl type prechamber", SAE paper No 2000-01-0587, SAE Transactions, Journal of Engines, Vol. 109, pp.718-733, 2000.
5. Watson, N and Marzouk, M., "A non-linear digital simulation of turbocharged diesel engines under transient conditions", SAE paper No 770123, 1977.
6. Winterbone, D.E., Benson, R.S., Mortimer, A.G., Kenyon, P. and Stotter, A., "Transient response of turbocharged diesel engines", SAE paper No 770122, 1977.
7. Watson, N., "Transient performance simulation and analysis of turbocharged diesel engines", SAE paper No 810338, 1981.
8. Bazari, Z., "Diesel exhaust emissions prediction under transient operating conditions", SAE paper No 940666, 1994.
9. Filipi, Z., Wang, Y. and Assanis, D., "Effect of variable geometry turbine (vgt) on diesel engine and vehicle system transient response", SAE paper No 2001-01-1247.
10. Rakopoulos, C.D. and Giakoumis, E.G., "Simulation and analysis of a naturally aspirated, indirect injection diesel engine under transient conditions comprising the effect of various dynamic and thermodynamic parameters", Energy Conversion and Management, Vol. 39, pp. 465-484, 1998.

11. Rakopoulos, C.D., Giakoumis, E.G. and Hountalas, D.T., "A simulation analysis of the effect of governor technical characteristics and type on the transient performance of a naturally aspirated IDI diesel engine", SAE paper No 970633, SAE Transactions, Journal of Engines, Vol. 106, pp. 905-922, 1997.
12. Rakopoulos, C.D., Giakoumis, E.G. and Hountalas, D.T., "Experimental and simulation analysis of the transient operation of a turbocharged multi-cylinder IDI diesel engine", Energy Research, Vol. 22, pp. 317-32, 1998.
13. Moran, M.J., "*Availability Analysis: A Guide to Efficient Energy Use*", New Jersey, Prentice Hall, 1982.
14. Moran, M.J. and Shapiro, H.N., "*Fundamentals of Engineering Thermodynamics*", John Wiley and Sons, New York, 1992.
15. Bejan, A., Tsatsaronis, G. and Moran, M., "*Thermal Design and Optimization*", John Wiley and Sons, New York, 1996.
16. Gyftopoulos, E.P. and Beretta, G.P., "Entropy generation rate in a chemically reacting system", Proceedings ASME-WAM, AES, Vol. 27 and HTD Vol. 228, Anaheim, CA, pp. 329-334, 1992.
17. Dunbar, W.R. and Lior, N., "Sources of combustion irreversibility", Combustion Science and Technology, Vol. 103, pp. 41-61, 1994.
18. Dunbar, W.R., Lior, N. and Gaggioli, R.A., "The component equations of energy and exergy", ASME Transactions, Journal of Energy Research and Technology, Vol. 114, pp. 75-83, 1992.
19. Flynn, P.F., Hoag, K.L., Kamel, M.M. and Primus, R.J., "A new perspective on diesel engine evaluation based on second law analysis", SAE paper No 840032, 1984.
20. McKinley, T.L. and Primus, R.J., "An assessment of turbocharging systems for diesel engines from first and second law perspectives", SAE paper No 880528, SAE Transactions, Journal of Engines, Vol. 97, pp. 1061-1071, 1988.
21. Van Gerpen, J.H. and Shapiro, H.N., "Second-law analysis of diesel engine combustion", ASME Transactions, Journal of Engineering for Gas Turbines and Power, Vol. 112, pp. 129-137, 1990.
22. Beretta, G.P. and Keck, J.C., "Energy and entropy balances in a combustion chamber", Combustion Science and Technology, Vol. 30, pp. 19-29, 1983.
23. Rakopoulos, C.D. and Andritsakis, E.C., "DI and IDI combustion irreversibility analysis", Proceedings ASME-WAM, AES Vol. 230 and HTD Vol. 266, New Orleans, LA, pp. 17-32, 1993.
24. Rakopoulos, C.D. and Kyritsis, D.K., "Comparative second-law analysis of internal combustion engine operation for methane, methanol, and dodecane fuels", Energy, Vol. 26, pp. 705-722, 2001.
25. Rakopoulos, C.D., Andritsakis, E.C. and Kyritsis, D.K., "Availability accumulation and destruction in a DI diesel engine with special reference to the limited cooled case", Heat Recovery Systems and CHP, Vol. 13, pp. 261-275, 1993.
26. Rakopoulos, C.D. and Giakoumis, E.G., "Speed and load effects on the availability balances and irreversibilities production in a multi-cylinder turbocharged diesel engine", Applied Thermal Engineering, Vol. 17, pp. 299-314, 1997.
27. Shapiro, H.N. and van Gerpen, J.H., "Two zone combustion models for second law analysis of internal combustion engines", SAE paper No 890823, 1989.
28. Rakopoulos, C.D., "Evaluation of a spark ignition engine cycle using first and second-law analysis techniques", Energy Conversion and Management, Vol. 33, pp. 1299-1314, 1993.
29. Caton, J.A., "Operating characteristics of a spark ignition engine using the second-law of thermodynamics: Effects of speed and load", SAE paper No 2000-01-0952.
30. Anderson, M.K., Assanis, D.N. and Filipi, Z.S., "First and second-law analyses of a naturally aspirated, Miller cycle SI engine with late intake valve closure", SAE paper No 980889, 1998.
31. Rakopoulos, C.D. and Giakoumis, E.G., "Development of cumulative and availability rate balances in a multi-cylinder turbocharged IDI diesel engine", Energy Conversion and Management, Vol. 38, pp. 347-369, 1997.
32. Lipkea, W.H. and deJoode, A.D., "A comparison of the performance of two direct-injection diesel engines from a second-law perspective", SAE paper No 890824, 1989
33. Caton, J.A., "A review of investigations using the second-law of thermodynamics to study internal combustion engines", SAE paper No 2000-01-1081.
34. Rakopoulos, C.D. and Giakoumis, E.G., "Simulation and exergy analysis of transient diesel engine operation", Energy, Vol. 22, pp. 875-886, 1997.
35. Whitehouse, N.D. and Way, R.G.B., "Rate of heat release in diesel engines and its correlation with fuel injection data", Proceedings of the Institution of Mechanical Engineers, Vol. 184, Part 3J, pp. 17-27, 1969-70.
36. Hiroyasu, H., Kadota, T. and Arai, M., "Development and use of a spray combustion modelling to predict diesel engine efficiency and pollutant emissions", Bulletin JSME, Vol. 26, pp. 569-576, 1983.
37. Rezeka, S.F. and Henein, N.A., "A new approach to evaluate instantaneous friction and its components in internal combustion engines", SAE paper No 840179, 1984.
38. Rakopoulos, C.D., Giakoumis, E.G. and Rakopoulos, D.C., "The effect of friction modelling on the prediction of turbocharged diesel engine transient operation", SAE paper No 2004-01-0925.
39. Rakopoulos, C.D., Giakoumis, E.G., Hountalas, D.T. and Rakopoulos, D.C., "The effect of various dynamic, thermodynamic and design parameters on the performance of a turbocharged diesel engine

operating under transient load conditions", SAE paper No 2004-01-0926.
40. Kouremenos, D.A., Rakopoulos, C.D., Hountalas, D.T. and Kotsiopoulos, P.N., "A simulation technique for the fuel injection system of diesel engines", Proceedings ASME-WAM, AES Vol. 24, Atlanta, GA, pp. 91-102, 1991.

NOMENCLATURE

A,a: exergy or availability, J
b: flow availability, J/kg
c_p: specific heat capacity, J/kg K
G: (mass) moment of inertia, kg m^2, or Gibbs free enthalpy, J
h: specific enthalpy, J/kg
I: irreversibility, J
m: mass, kg
N: engine speed, rpm
p: pressure, Pa
Q: heat, J
S: entropy, J/K
s: specific entropy, J/kg K
T: absolute temperature, K, or torque,N m
t: time, s
U: internal energy, J
V: volume, m^3
z: fuel pump rack position, m

Greek
η_m: mechanical efficiency
λ: gas thermal conductivity, W/m K
φ: crank angle, deg or rad
ω: angular velocity, s^{-1}

Subscripts
O: atmosphere conditions
1: compressor inlet
2: compressor outlet
3: aftercooler outlet
4: inlet manifold
5: cylinder
6: exhaust manifold
7: turbine outlet
C: compressor
ch: chemical
cw: cooling water
e: engine
em: exhaust manifold
fb: fuel burning
fr: friction
g: gas
im: inlet manifold
j: any cylinder
L: load or loss
TC: turbocharger
T: turbine
tot: total
w: wall or work

Abbreviations
^{o}CA: degrees of crank angle
rpm: revolutions per minute